

ORIGIN OF THE FAR OFF-AXIS GRB171205A

SHLOMO DADO¹ AND ARNON DAR¹

¹*Physics Department, Technion, Haifa 32000, Israel*

ABSTRACT

We show that observed properties of the low luminosity GRB171205A and its afterglow, like those of most other low-luminosity gamma ray bursts (LL-GRBs), indicate that it is an ordinary SN-GRB, which was produced by inverse Compton scattering of glory light by a highly relativistic narrowly collimated jet ejected in supernova (SN) explosion and viewed from a far-off axis angle. However, only VLA/VLBI follow-up radio observations of a superluminal displacement of its radio afterglow from its parent supernova, and/or measurements of its late-time X-ray afterglow with the Chandra X-ray observatory will be able to disprove that it was powered by a nascent pulsar in the SN explosion.

1. INTRODUCTION

The standard fireball model of gamma ray bursts (GRBs) cannot explain a difference of 6 orders of magnitude in luminosity between ordinary GRBs such as 130427A and nearby low luminosity (LL) GRBs, such as 980425 and 060218, if they belong to the same population of GRBs, as indicated by their association with similar supernovae (e.g., Melandri et al. 2014). Neither could it explain the much larger GRB production rate relative to the star formation rate of LL GRBs than that of ordinary GRBs. This led many authors to propose that ordinary GRBs and LL GRBs belong to different populations of GRBs (e.g., Toma et al. 2007; Liang et al. 2007; Guetta & Della Valle 2007; Virgili et al. 2009; Bromberg et al. 2012), which has been widely accepted.

In contrast, in the cannonball model of GRBs, LL SN-GRBs and LL SN-less GRBs are ordinary GRBs observed from far off-axis viewing angles (Dar & De Rújula, 2000a, 2004; Dado, Dar & De Rújula 2003, 2009; Dado & Dar 2017) whose rates depend on viewing angle and detection threshold. When their effects are properly included, the extracted GRB rate from the observed rate as function of redshift becomes proportional to the star formation rate at all redshifts (Dado & Dar 2014). This conclusion, however, for very small redshifts was based on very few LL SN-GRBs and LL SN-less GRBs.

Recently the LL GRB171205A, was detected by the Swift Burst Alert Telescope (BAT) (D’Elia et al. 2017). It was located by the Swift X-ray Telescope (XRT) in a nearby bright spiral galaxy (Izzo et al. 2017a) of redshift $z = 0.0368$ (Izzo et al. 2017b). Assuming a standard cosmology model with $H_0 = 70$ km/s/Mpc, $\Omega_M = 0.30$, and $\Omega_\Lambda = 0.70$, the burst isotropic energy release E_{iso} as measured by Konus Wind (Frederiks et al. 2017) was 2.4×10^{49} erg in the 20-1500 keV range. So far, only limited evidence for the association of GRB171205A with a bright SN was reported (Ugarte Postigo et al. 2017; Cobb 2017). However, the observed properties of GRB171205A and its afterglow can be used already to further test whether it was an ordinary SN-GRB viewed from a far off-axis angle, or was it a member of a different population of GRBs.

2. LL GRBS IN THE CB MODEL

In the cannonball (CB) model (Dar & De Rújula 2004) of GRBs, ordinary long duration GRBs are produced by inverse Compton scattering (ICS) of glory light (a light halo surrounding the GRB site) by highly relativistic jets of plasmoids (CBs) of ordinary matter (Shaviv & Dar 1995) launched in stripped envelope supernova explosions (Dar et al. 1992) and in phase transition of neutron stars to quark stars (Shaviv & Dar 1995; Dado

& Dar 2017). In the CB model, ordinary GRBs are viewed from an angle $\theta \approx 1/\gamma$ relative to the jet direction of motion, while low luminosity (LL) GRBs and X-ray flashes (XRFs) are ordinary GRBs viewed from far off-axis, $\gamma^2\theta^2 \gtrsim 9$. Both ordinary GRBs and LL GRBs were predicted to display simple kinematical correlations between their main properties (Dar & De Rújula 2000a). E.g., the peak energy of their time integrated energy spectrum satisfies $(1+z)Ep \propto \gamma\delta$, while their isotropic equivalent total gamma ray energy satisfies $E_{iso} \propto \gamma\delta^3$, where z is their redshift and $\delta = 1/\gamma(1 - \beta \cos\theta)$ is their Doppler factor. Hence, ordinary GRBs that are mostly viewed from an angle $\theta \approx 1/\gamma$, were predicted to satisfy

$$(1+z)Ep \propto [E_{iso}]^{1/2}, \quad (1)$$

while far off-axis ($\theta^2\gamma^2 \gg 1$) GRBs and SHBs were predicted to satisfy (Dar & De Rújula 2000a, Eq.(40))

$$(1+z)Ep \propto [E_{iso}]^{1/3}. \quad (2)$$

Eqs.(1) and (2) are compared in Figure 1 and 2 to the observational data on GRBs with known z , Ep and E_{iso} . As can be seen from Figure 1, the CB model predicted correlation for ordinary GRBs as given by Eq.(1), which was later discovered empirically by Amati et al. (2002) and repeatedly tested by Amati et al. (2006, 2008, 2009, 2013) and by many other authors, is well satisfied by ordinary ($\theta \sim 1/\gamma$) GRBs. As can be seen from Figure 2, Eq.(2), the CB model predicted correlation for far off-axis GRBs ($\theta\gamma \gg 1$), is also well satisfied by the LL-GRBs. E_{iso} of the LL GRB171205A is indicated in Figure 2 by an arrow. From the correlation shown in Figure 2 we estimate its $Ep \approx 79$ keV, and from the CB model relation (e.g., Dar & De Rújula 2004)

$$Ep = \frac{\gamma\theta\epsilon}{(1+z)} \approx \frac{2\epsilon}{\theta^2(1+z)} \quad (3)$$

for $\gamma^2\theta^2 \gg 1$ and a mean energy of glory photons, $\epsilon \sim 1$ eV, we estimate a far off-axis viewing angle $\theta \approx \sqrt{2/79(1+z)} \approx 5 \times 10^{-3}$, which we shall assume hereafter in our analysis of the observations of GRB171205A.

3. PULSE SHAPE

In the cannonball (CB) model (Dar & De Rújula 2004), the production mechanism of GRBs is ICS of photons of a glory (light fireball) of radius R surrounding the launching site of a highly relativistic jet of plasmoids (bulk motion Lorentz factor $\gamma \sim 10^3$). The glory has a bremsstrahlung spectrum of temperature T , which yields a FRED (fast rise exponential decay) pulse shape of photons above a detection threshold E_{min} ,

$$N(t, E > E_{min}) \propto \frac{t^2}{(\Delta^2 + t^2)^2} \exp(-t/\tau) \quad (4)$$

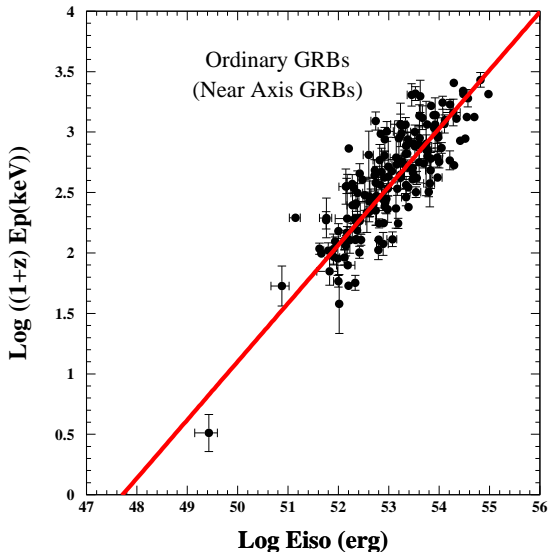


Figure 1. The peak energy in the GRB rest frame as a function of the isotropic equivalent total gamma ray energy of ordinary GRBs viewed near axis. The line is the correlation predicted by the CB model as given by Eq.(1).

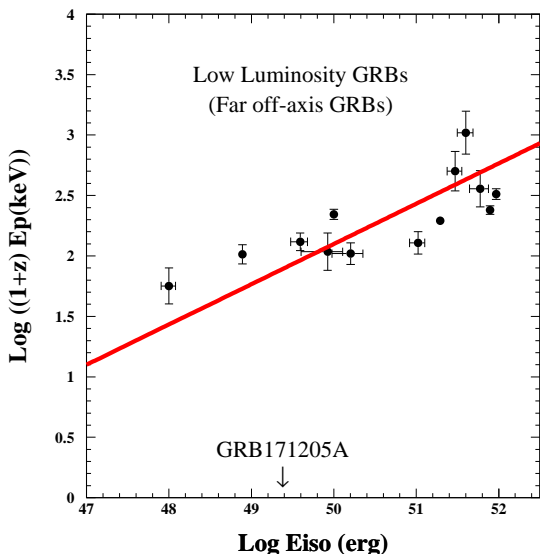


Figure 2. The peak energy in the GRB rest frame as a function of the isotropic equivalent total gamma ray energy E_{iso} of low luminosity (far off-axis) GRBs. The line is the correlation predicted by the CB model, as given by Eq.(2) for far-off axis (low luminosity) GRBs.

where $\tau(E_{min}) = (R/\gamma c)(kT E_{min})$ and Δ are best fit parameters. $\sim t^2$ rise in Eq.(4) is a simple interpolation between the early-time rise due to the increasing effective cross section of the CB $\pi R_{CB}^2 \propto t^2$

while it is crossing inside the glory region where the ambient photons are isotropic and the late-time behavior $\sim (1/t^2) \exp(-t/\tau)$ when the CB is at a distance $r = \gamma \delta ct / (1+z) \gg R$ from its launch site, whose derivation is as follows:

At distances $r \gg R$ the number density of ambient photons intercepted by the CB decreases with distance as $1/r^2 \propto t^{-2}$ and hence

$$\frac{dn}{d\epsilon} \propto t^{-2} \exp(-\epsilon/kT)/\epsilon. \quad (5)$$

In the CB's rest frame, the longitudinal momentum of the intercepted photons is reduced by a factor $1/2\gamma$. Thus, in that frame, the photon's parallel momenta are negligible compared to their transverse momenta, unchanged by the Lorentz boost. Let b be the transverse distance of an emitted photon relative to the CB's direction of motion, which is intercepted at $r \gg R$. Its energy in the CB rest frame becomes $\epsilon' \approx \epsilon b/r$ and after ICS in the CB it arrives with $E \approx \epsilon \delta b/r(1+z) = \epsilon b/\gamma ct$ in the observer frame. Hence, the photon flux above the detection threshold E_{min} as seen by the distant observer is given by

$$N(t, E > E_{min}) \propto R_{CB}^2 \int_{E_{min}}^{\infty} \int_0^R \frac{dn}{d\epsilon} \frac{d\epsilon}{dE} 2\pi b db dE \quad (6)$$

which yields the late-time pulse shape in the limit $t \gg \tau$.

4. THE X-RAY AFTERGLOW

The afterglow observations with the Swift X-ray telescope (XRT) in the 0.3-10 keV range begins usually during the fast decline phase of the prompt emission. The energy flux above E_{min} due to ICS during this phase is given similarly by

$$F(E > E_{min}) = \int E \frac{dN}{dE} dE \propto t^{-2} \exp(-t/\tau(E_{min})). \quad (7)$$

The E-dependence of $\tau(E) = (R/\gamma c)(kT E)$ produces the fast spectral softening observed during the fast decline phase of the prompt emission pulses (Evans et al. 2007; 2009). In SN-GRBs, this fast decline phase is overtaken by synchrotron radiation from the decelerating jet in the relatively high density interstellar environment (e.g., a molecular cloud, where most SNeIc usually take place). In SN-Less GRBs, the fast decline phase is overtaken by an afterglow produced by a plerion powered by a millisecond pulsar which underwent a phase transition (to a quark star ?) due to mass accretion in a compact binary (Dado & Dar 2017).

In a constant density ISM, this deceleration yields (Dado, Dar & De Rújula 2009a; Dado & Dar 2014)

$$\gamma(t) = \frac{\gamma(0)}{[\sqrt{(1 + \gamma(0)^2 \theta^2)^2 + t/t_s - \gamma(0)^2 \theta^2}]^{1/2}} \quad (8)$$

and

$$F(E, t) \propto [\gamma(t)]^{3\beta-1} [\delta(t)]^{\beta+3} \nu^{-\beta} \quad (9)$$

where β is the spectral index of the X-rays. Eq.(9) yields a late-time power-law decline (e.g. Dado & Dar 2016) $F(E, t) \rightarrow \nu^{-\beta} t^{-\beta-1/2}$.

A plerion powered by a pulsar with a period P and period derivative \dot{P} produces an afterglow with a light curve $F \propto F_{ps}(1 + t/t_b)^{-2}$ (Dado & Dar 2017) where a transition from a plateau to $\sim t^{-2}$ decrease takes place around $t_b = P/2\dot{P}$.

In Figures 3 and 4 the light curve of the X-ray afterglow of GRB171205A, that was measured with the Swift XRT and reported in the Swift-XRT GRB lightcurve repository (Evans et al. 2007,2009) is compared to the CB model best fit lightcurves for a fast declining ICS emission (Eq.(7)) taken over the synchrotron emission from a decelerating jet in a constant density ISM (Eq.(9)), or by X-ray emission from a plerion powered by a pulsar, respectively. The prompt emission involved only two adjustable parameters, a normalization and $\tau(E_{min})$. The synchrotron afterglow involved only two adjustable parameters, a normalization and a deceleration time $t_s = 387$ s. The viewing angle $\theta = 5$ mrad was obtained from *Eiso*, and the spectral index of the X-ray afterglow, $\beta \approx 0.92$ was that measured with Swift. The pulsar powered afterglow fit involved only two adjustable parameters, a normalization and $t_b = 4.5$ days, which yielded $P \sim 145$ ms and $\dot{P} \sim 1.86 \times 10^{-7}$ (Dado & Dar 2017). The two best fits have comparable χ^2/dof , 1.31 and 1.38, respectively, which cannot distinguish yet between a jet afterglow and a pulsar powered afterglow.

5. SUPERLUMINAL MOTION

A very specific prediction of the CB model (Dar & De Rújula 2000b; Dado, Dar & De Rújula 2003, 2016) is an apparent superluminal velocity of the afterglow of SN-GRBs in the plane of the sky, which is given by

$$V_{app} \approx \frac{2\gamma^2 c \theta}{(1 + \gamma^2 \theta^2)(1 + z)}. \quad (10)$$

In far-off axis SN-GRBs, $V_{app} \approx 2c/(1+z)\theta$ as long as $\gamma^2 \theta^2 \gg 1$, i.e., $t \ll t_b = (1 + \gamma_0^2 \theta^2)^2 t_s$, and $V_{app} \propto t^{-1/2}$ for $t \gg t_b$. In the case of a plerion afterglow, no separation between the GRB and its afterglow is expected. In Figures 5,6 we present a plot of the apparent superluminal velocity of the afterglow of GRB171205A in the plane of the sky and the angular displacement of the afterglow from the burst position, respectively, as predicted by the CB model. The viewing angle $\theta \approx 5$ mrad and the deceleration time scale $t_s \approx 387$ s are those

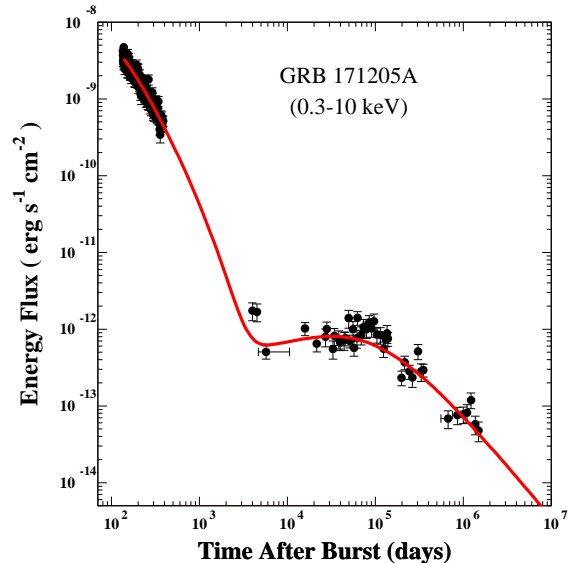


Figure 3. The light curve of the X-ray afterglow of GRB171205A reported in the Swift-XRT GRB lightcurve repository (Evans et al. 2007,2009) compared to the afterglow predicted by the CB model, assuming a far-off axis ordinary SN-GRB.

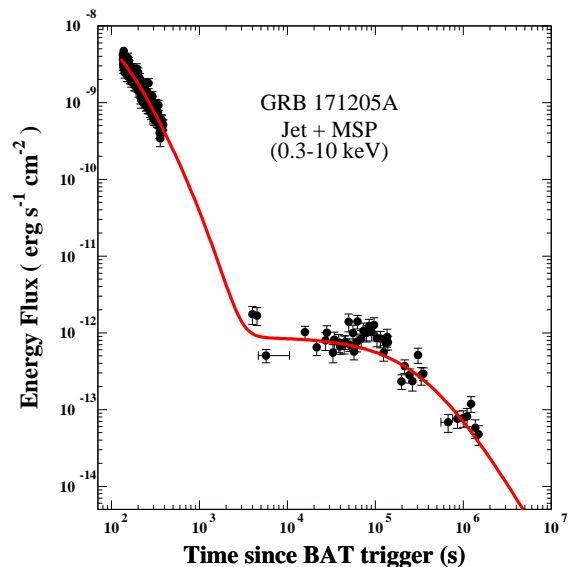


Figure 4. The light curve of the X-ray afterglow of GRB171205A reported in the Swift-XRT GRB lightcurve repository (Evans et al. 2007,2009) compared to the predicted decay by the CB model of its prompt emission taken over by plerion emission powered by a nascent pulsar.

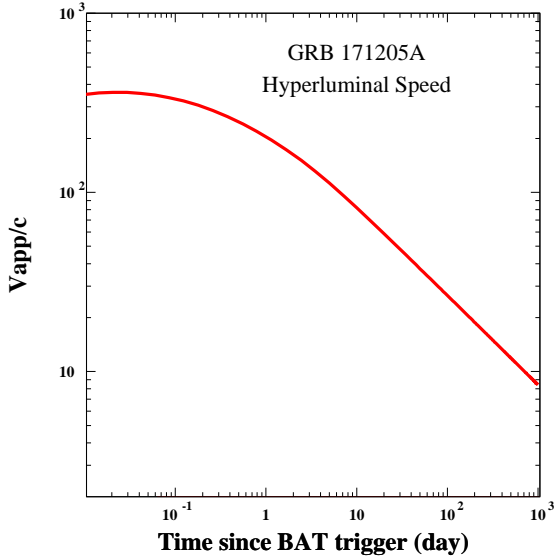


Figure 5. The expected superluminal velocity of the highly relativistic jet, which produced the LL GRB171205A, as function of time, based on the parameters of the best fit CB model lightcurve to its X-ray afterglow.

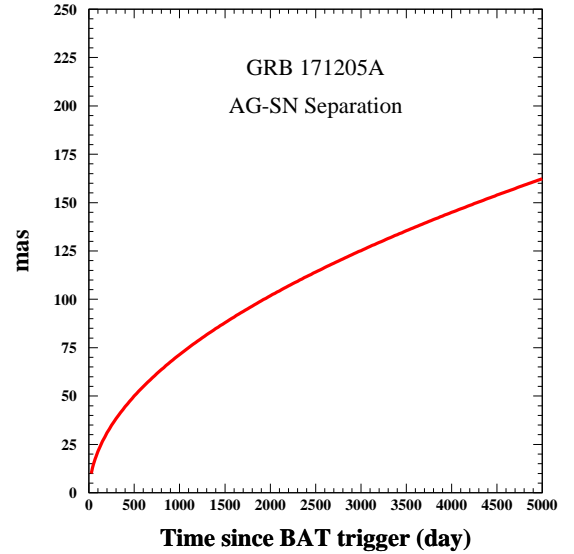


Figure 6. The angular separation between the afterglow of GRB171205A and the GRB-SN location as function of time after burst expected in the CB model from the parameters of the highly relativistic jet extracted from the lightcurve of the X-ray afterglow of GRB171205.

used to reproduce the light curve of X-ray synchrotron afterglow shown in Figure 3.

6. CONCLUSION

The observations of the low luminosity GRB171205A and its afterglow analyzed in the framework of the cannonball model of GRBs, indicate that it is an ordinary SN-GRB viewed from far off-axis. like all other LL GRBs.

REFERENCES

- Amati, L., Frontera, F., Tavani, M., et al. 2002, *A&A*, 390, 81 [arXiv:astro-ph/0205230]
- Amati, L., 2006, *MNRAS*, 372, 233 [arXiv:astro-ph/0601553]
- Amati, L., Frontera, F., Guidorzi, C. 2009, *A&A*, 508, 173 [arXiv:0907.0384]
- Amati, L., Della Valle, M., 2013, *IJMP D*, 22, 1330028 [arXiv:1310.3141]
- Bromberg, O., Nakar, E., Piran, T., Sari, R., 2012, *ApJ*, 749, 110 [arXiv:1111.2990]
- Cobb, B. E., 2017, *GCN* 22270
- Dado, S. & Dar, A., 2014, *ApJ*, 785, 70 [arXiv:1307.5556]
- Dado, S. & Dar, A., 2016, *PRD*, 94, 063007 (2016) [arXiv:1603.06537]
- Dado, S. & Dar, A., 2017, arXiv:1710.02456
- Dado, S., Dar, A., De Rújula, A., 2003 *A&A*, 401, 243 [arXiv:astro-ph/0309294]
- Dado, S., Dar, A., De Rújula, A., 2009, *ApJ*, 696, 994 [arXiv:0809.4776]
- Dado, S., Dar, A., De Rújula, A., arXiv:1610.01985
- Daigne, F., & Mochkovitch, R., 2007, *A&A*, 465, 1 [arXiv:0707.0931]
- Dar, A., & De Rújula, 2000a, arXiv:astro-ph/0008474.
- Dar, A. & De Rújula, A., 2000b [arXiv:astro-ph/0012227]
- Dar, A. & De Rújula, A., 2004, *PhR*, 405, 203 [arXiv:astro-ph/0308248]
- Dar, A., Kozlovsky, Ben Z., Nussinov, S., Ramaty, R., 1992, *ApJ*, 388, 164
- D’Elia, V., D’Ai, A., Lien, A. Y., Sbarufatti, B., et al. 2017, *GCN* 22127
- Evans, P. A., Beardmore, A. P., Page, K. L., et al., 2007, *A&A*, 469, 379 [arXiv:0704.0128]
- Evans, P. A., Beardmore, A. P., Page, K. L., et al., 2009 *MNRAS*, 397, 1177 [arXiv:0812.3662]
- Frederiks, D, Golenetskii, S., Aptekar, R., et al. 2017, *GCN* 22227
- Guetta, D., Della Valle, M., 2007, *ApJ*, 657, L76
- Izzo, L., D. A. Kann, D. A., Fynbo, J. P. U., et al. 2017a, *GCN* 22178
- Izzo L., Selsing, S., Japelj, J., et al. 2017b, *GCN* 22180
- Melandri, A., E. Pian, E., D’Elia, V., et al. *A&A*, 567, A29 (2014) [arXiv:1404.6654].
- Shaviv, N. & Dar, A., 1995, *ApJ*, 447, 863 [arXiv:astro-ph/9407039]
- Toma, K., Ioka, K., Sakamoto, T., Nakamura, T., 2007, *ApJ*, 659, 1420 [arXiv:astro-ph/0610867]
- Ugarte Postigo, A., Izzo, L., D.A. Kann, D. A., et al. 2017, *GCN* 22204
- Virgili, F. J., Liang, E., ; Zhang, B., 2009, *MNRAS*, 392, 91 [arXiv:0801.4751]